applied sciences

MDPI

Article

Electrons and X-rays to Muon Pairs (EXMP)

Camilla Curatolo * and Luca Serafini

INFN Sezione di Milano, via Celoria 16, 20133 Milan, Italy; luca.serafini@mi.infn.it

* Correspondence: camilla.curatolo@mi.infn.it

Abstract: One of the challenges of future muon colliders involves the production of muon beams carrying high phase space densities. In particular, the muon beam normalised transverse emittance is a relevant figure of merit used to meet luminosity requests. A typical issue impacting the achieved transverse emittance in muon collider schemes, thus far considered, is the phase space dilution caused by the Coulomb interaction of primary particles propagating into the target where muons were generated. In this study, we present a new scheme(named electrons and X-rays to muon pairs) for muon beam generation occurring in a vacuum via interactions of electron and photon beams. Setting the center of mass energy at about twice the threshold (i.e., around 350 MeV), the normalised emittance of the muon beam generated via muon pair production reaction ($e^- + \gamma \rightarrow e^- + \mu^+ + \mu^-$) is largely independent on the emittance of the colliding electron beam and is set basically by the excess of transverse momentum in the muon pair creation. In absence of any other mechanism for emittance dilution, the resulting muon beam, with energy in the range of a few tens of GeV, is characterised by an ultra-low normalised transverse RMS emittance of a few nm rad, corresponding to a geometrical emittance below 10 π pm rad. This opens up the way to a new muon collider paradigm based on muon sources conceived with primary colliding beams delivered by 100 GeV-class energy recovery LINACs interacting with hard-X ray free electron lasers. The challenge is to achieve the requested luminosity of the muon collider adopting a strategy of low muon fluxes/currents combined to ultra-low emittances, to largely reduce the levels of muon beam-induced backgrounds.

Keywords: muon collider; high efficiency XFEL; FELs for colliders; low emittance muon beam photoproduction

check for updates

Citation: Curatolo, C.; Serafini, L. Electrons and X-rays to Muon Pairs (EXMP). *Appl. Sci.* **2022**, *12*, 3149. https://doi.org/10.3390/app12063149

Academic Editor: Wolfram Helml

Received: 5 February 2022
Accepted: 16 March 2022
Published: 19 March 2022

1. Introduction

Muon beam generation for muon colliders has been traditionally conceived using hadronic interactions that go through a pion production channel with consequent decay into the muons. The total cross section for these reactions is quite large, assuring a wealth of muon populations when intense proton beams are impinging on targets made of proper material [1]. Unfortunately, the coulomb interactions of primary and secondary beams into the target largely disrupt the phase space of the generated muon beam, diluting its emittance well above the upper limits set by collider luminosity requests, so that a challenging muon cooling process must be implemented via ionisation with the aim to restore the emittance levels down to values compatible of collider luminosity [2]. Alternatively, positron-electron annihilation into muon pairs has been proposed as a promising scheme to achieve low emittance values directly at the muon source [3]. Investigations into this scheme are still in progress, to assess its full potentiality; nevertheless, the primary beam of 45 GeV positrons has to interact with a solid target in order to achieve a sufficient muon pair production rate, which in turns poses issues of target handling. An exotic scheme of the hadron photon collider (HPC) was proposed to generate muon pairs through the reaction $p^- + \gamma \rightarrow p^- + \mu^+ + \mu^-$. In this case, the emittance of the muon beam was quite good, basically conserving the emittance of colliding proton and photon beams [4–6]. The very small, total cross section typical of muon photo-production reactions sets a severe limit to the muon flux achievable. In this paper, we revisit the basic concepts of that study, implementing the idea of muon photo-production in a different environment, that of electron-photon collisions, with the scheme electrons and X-rays to muon pairs (EXMP). The reason why pertains not really to the larger cross section of the e, γ reaction, with respect to p, γ (the increase is quite modest), but in the possibility of running an electron-photon collider at a much larger luminosity than a proton-photon collider, such as in the HPC scheme. The focal spot size of a 100-GeV-class electron beam colliding in-vacuum with a counterpropagating photon beam can be much smaller than that of a TeV proton beam stored in a machine, such as LHC, as well as that of an electron-positron collider final focus. The former is actually limited by the minimum beta achievable in a proton storage ring due to cm-long proton bunches, the latter is actually limited by the beam-beam interaction, originated by the presence of colliding charged particles, focused into a tight focal region. In cases of electron-photon collisions, none of these effects are actually present since electrons and photons interact through two-particle QED reactions without a significant collective e.m. field effect impacting the beam propagation through the interaction region. Thus, the maximum focus achievable in the collision region is dictated by the final focus beam optics, electron and photon bunch lengths, and transverse emittances of the two colliding beams. In order to reach center of mass (CM) energies in excess of 300 MeV to which the muon pair production total cross section exceeds a few hundred nano barns, we were forced to consider electrons with energies higher than 200 GeV and photons with energy in the 60–150 keV range. Following the analysis pursued in HPC studies, in order to maximise the luminosity of an electron-photon collider in this range of the particle-photon energies, we considered a hard X-ray free electron laser (FEL) as the brightest radiation source and an energy recovery LINAC (ERL) to obtain the maximum electron beam current (A-class), combined with high brightness, namely short electron bunches (fs-class) with very small transverse normalised emittances (below 1 mm mrad). Since no concern was raised by the beam-beam interaction effects, maximum luminosity was achieved running round beams at the collision, aiming at minimum beta values at the final focus. In the following, we will show that (near) state-of-the-art performances, both of FELs and ERLs, indicate the possibility of achieving an outstanding luminosity in the $e^- - \gamma$ collider, up to 10^{42} cm^{-2}s^{-1}, which allow generating up to 10^{11} muon pairs per second with geometrical emittances down to 5 π pm rad. The paper is organised as follows: in Section 2, we summarize the theoretical aspects regarding the electron-photon beam collisions, and the main formulas to analyse the $e^- - \gamma$ scheme reported in Section 3. In the latter, we discuss the performance requests to primary beams, how to achieve the requested performances running dedicated ERLs to drive the hard X-ray FEL (Section 3.1), and the power consumption demands (Section 3.2). Section 4 is dedicated to the results of Monte Carlo simulations to assess the phase space distributions and the quality of the generated muon beams, its flexibility, and dynamic range. A proof of principle (PoP) experiment to validate the proposed scheme is described in Section 5. The conclusions roughly depict the way towards a TeV muon collider based on an $e^- - \gamma$ collider muon source.

2. Theory

Here, we analyse the most important aspects concerning the electron-photon beam collisions at the center of mass energy, around 350 MeV.

The center of mass energy is given by $E_{CM} = \sqrt{2E_e h\nu - 2(\underline{p}_e \cdot \underline{k}) + M_e^2}$ where E_e, $\underline{p}_e$ and $h\nu$, $\underline{k}$ are electron and photon energies and momenta, respectively, and $M_e = 0.511$ MeV/c^2 is the electron mass (natural units are used i.e., c = 1). Assuming a head-on collision within the electron and the incident photon with energy $h\nu << E_e$ and supposing $M_e^2 << E_e h\nu$, the Lorentz factor of the center of mass is

$$\gamma_{CM} = \frac{E_{tot}^{LAB}}{E_{CM}} \simeq \frac{E_e + h\nu}{\sqrt{4E_e h\nu + M_e^2}} \simeq \frac{E_e}{2\sqrt{E_e h\nu}} = \frac{\sqrt{E_e}}{2\sqrt{h\nu}}. \quad (1)$$

The CM threshold energy for the muon pair production (MPP) is given by $E^{th}_{CM} = M_e + 2M_\mu$. If for example $E_e = 200$ GeV, the equality $M_e + 2M_\mu = \sqrt{4E_e h\nu + M_e^2}$ implies that $h\nu^{th} = 56.6$ keV. The photon energy in the electron rest frame is $h\nu^{th'} = 2\gamma_e h\nu^{th} = 44.3$ GeV, while the photon energy in the CM frame is $h\nu^{th*} = 2\gamma_{CM} h\nu^{th} = 106.5$ MeV.

Besides MPP, the other predominant reactions in the mentioned CM energy range are triplet pair production (TPP—$e^- + \gamma \rightarrow e^- + e^+ + e^-$) and inverse Compton scattering (ICS - $e^- + \gamma \rightarrow e^- + \gamma$).

The electron recoil parameter, defined as

$$X = 2h\nu'/M_e = 4\gamma_e h\nu/M_e, \tag{2}$$

achieves very high values in the cases of our interest (in the order of 10^5). We also notice the center of mass energy scales, such as the square root of X: $E_{cm} \simeq M_e\sqrt{1+X}$.

The TPP cross section, calculated as in reference [7], is

$$\sigma^{TPP}_{tot} = \sigma^{TPP}_{Bethe-Heitler} - \sigma^{TPP}_{Borsellino}$$

$$\begin{cases} \sigma^{TPP}_{Bethe-Heitler} = \alpha r_e^2[3.11\ \ln(X) - 8.07] \\ \sigma^{TPP}_{Borsellino} = \frac{2\alpha r_e^2}{X}\left[\frac{4}{3}\ \ln^3(X) - 3\ \ln^2(X) + 6.84\ \ln(X) - 21.51\right] \end{cases} \tag{3}$$

where $\alpha \simeq 1/137$ is the fine-structure constant and $r_e^2 = 0.079$ barn is the classical electron radius squared.

In a similar way, the MPP cross section can be obtained from the one above by substituting r_e with $r_\mu = r_e(M_e/M_\mu)$ and X with $X(M_e/M_\mu)$.

The ICS cross section is given by [8]

$$\sigma^{ICS}_{tot} = 2\pi r_e^2 \frac{1}{X}\left[\left(1 - \frac{4}{X} - \frac{8}{X^2}\right)\ln(1+X) + \frac{1}{2} + \frac{8}{X} - \frac{1}{2(1+X)^2}\right]. \tag{4}$$

The total cross sections σ_{tot} as a function of E_{CM} are depicted in Figure 1.

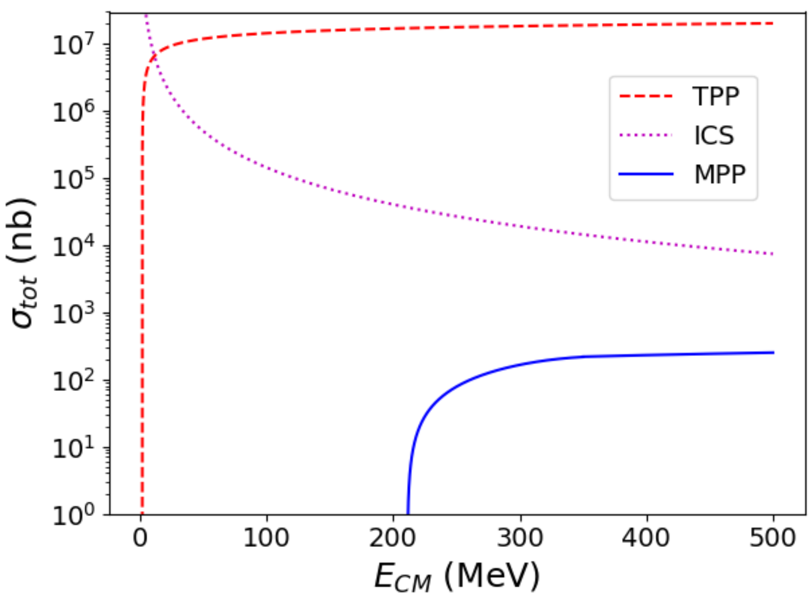

Figure 1. Total cross sections of predominant reactions in the electron–photon collision as a function of E_{cm} (MeV): muon pair production (MPP—$e^- + \gamma \rightarrow e^- + \mu^+ + \mu^-$), triplet pair production (TPP—$e^- + \gamma \rightarrow e^- + e^+ + e^-$), and inverse Compton scattering (ICS—$e^- + \gamma \rightarrow e^- + \gamma$).

The luminosity of the $e^- - \gamma$ collider is defined as

$$\mathcal{L} = \frac{N_e\, N_{ph}\, r}{2\,\pi\,\sqrt{\sigma_{x_e}^2 + \sigma_{y_e}^2}\sqrt{\sigma_{x_{ph}^2} + \sigma_{y_{ph}}^2}}\;[\mathrm{cm}^{-2}\,\mathrm{s}^{-1}] \quad (5)$$

with N_e, N_{ph} being the number of electron and photons per bunch, r the repetition rate of the collisions, and $\sigma_{x_e}, \sigma_{y_e}, \sigma_{x_{ph}}, \sigma_{y_{ph}}$ the transverse dimensions of the electron and the photon beams, respectively. The number of muon and electron pairs and ICS events per second can be obtained by multiplying the primary collider luminosity by the respective total cross sections.

The transverse normalised emittance of the produced muon is determined by the intrinsic thermal contribution of the reaction and by the features of the incoming electron beam. It can be described by an ad-hoc formula that we developed following the derivation reported in reference [6], (Equations (5) and (6)), whose first member is the product of the RMS muon beam size times the RMS muon beam transverse momentum due to the excess energy available in the reaction ($E_{cm} > E_{cm}^{th}$), while the second member of the formula represents the contribution of the electron beam RMS divergence angle at the interaction point:

$$\epsilon_\mu^n \simeq \frac{2}{3}\sigma_0 \frac{\sqrt{E_e\, h\nu} - M_\mu}{M_\mu} + \frac{\langle\gamma_\mu\rangle \epsilon_e^n}{\gamma_e} \quad (6)$$

where $\sigma_0 = \sqrt{\left(\sqrt{\sigma_{x_e}^2 + \sigma_{y_e}^2}\sqrt{\sigma_{x_{ph}}^2 + \sigma_{y_{ph}}^2}\right)/2}$, ϵ_e^n is the incoming electron beam transverse normalised emittance, $\langle\gamma_\mu\rangle$ the mean energy of the muon beam. By using the definition of the recoil parameter X, Equation (6) can be cast in a different form, better underlying the role of X:

$$\epsilon_\mu^n \simeq \frac{2}{3}\sigma_0 \left(\frac{M_e}{2M_\mu}\sqrt{X} - 1\right) + \frac{\epsilon_e^n}{\sqrt{X}} \quad (7)$$

with $X > X^{th} \simeq \frac{4M_\mu^2}{M_e^2} = 1.8 \times 10^5$. It clearly shows that primary collisions with photon beams operating at very large recoil factors generate muon beams whose emittances are independent of the primary particle colliding beam. EXMP is run at recoil factors of about 5×10^5, while HPC (see references [4–6]) is run at small recoil factors. This is the basic reason why EXMP achieves ultra-small emittance in the generated muon beams. The emittance reduction of a secondary beam produced in high recoil electron-photon collisions has already been identified and discussed in Equations (13), (14), and (23) of reference [8].

3. $e^- - \gamma$ Collider Scenarios

We conceived a novel $e^- - \gamma$ collider scenario achieving ultra-high luminosity. An overarching goal is the quest of very high sustainability: such luminosity levels typically require beam power levels that are hardly compatible with reasonable impacts on society and governmental approvals when power consumption of the whole scenario exceeds the so-called GW scale, which should be considered an unsurpassable borderline. The resulting criterion for the choice of the electron accelerators is the following: since the generation of muon pairs in the collision between the primary electrons and the FEL photons is perturbative on the primary beams, with negligible losses of beam particles and very small energy loss in the beams, a strategy for beam power recovery is mandatory. The scenario we have conceived, named EXMP, is based on PERLE-like ERLs [9,10]) and ILC schematics [11,12]. A representation is sketched in Figure 2 and two working points (WP200, WP500), corresponding to the dynamic limits of the parameters, are reported in Table 1.

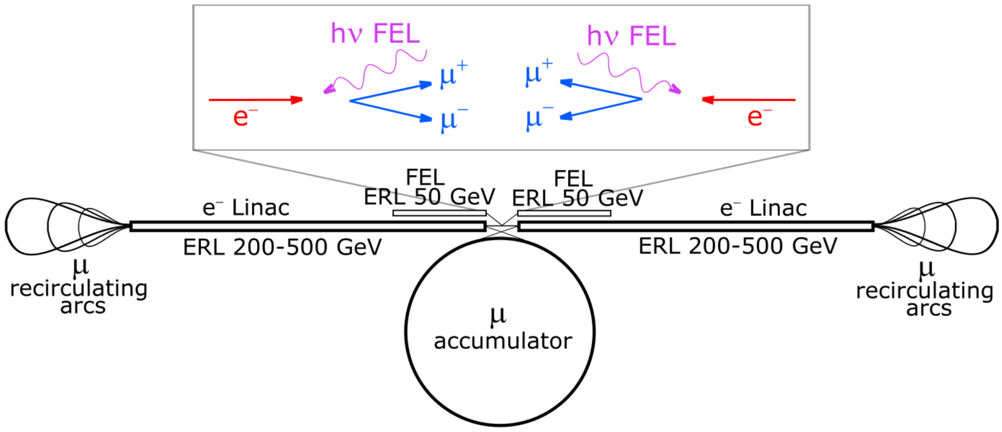

Figure 2. EXMP scheme. Primary e^-, accelerated up to 200–500 GeV, collide with the counterpropagating FEL, producing $\mu^\pm$. Both e^- (primary and FEL) are decelerated in the opposite LINACs and the energy recovered. A selected fraction of $\mu^\pm$ is injected in the opposite LINAC and accelerated before storage and collision in a ring.

Table 1. Parameters table of the EXMP scenario at two working points (WP200, WP500). Primary beam features and peak luminosities are reported.

	EXMP WP200	**EXMP WP500**
Energy e^- beam (GeV)	200	500
Bunch charge (pC)	250	250
Electrons per bunch (10^9)	1.6	1.6
Repetition rate (MHz)	800	800
Average current (mA)	2 × 200	2 × 200
Nominal beam power (GW)	2 × 40	2 × 100
Beam power recovery fraction (%)	99.9	99.95
Beam power loss (MW)	2 × 40	2 × 50
Bunch length (psec)	0.3	0.2
$\epsilon^n_{x,y}$ (π µm rad)	0.4	0.4
$\beta_{x,y}$ (mm)	0.2	0.23
$\sigma_{x,y}$ (nm)	14	10
FEL photon energy (keV)	150	60
Photons per pulse (10^{12})	5	12.5
$\epsilon_{x,y}$ (π pm rad)	0.6	1.5
Focal spot size (nm)	14	10
Repetition rate (MHz)	800	800
FEL beam power (MW)	2 × 100	2 × 100
FEL ρ (10^{-4})	5	8
FEL efficiency (tapering) (%)	1	1
FEL e^- beam average current (mA)	200	200
FEL e^- beam bunch charge (pC)	250	250
FEL e^- beam energy (GeV)	50	50
FEL e^- beam power (GW)	2 × 10	2 × 10
Beam power recovery fraction (%)	99.9	99.9
Beam power loss (MW)	2 × 10	2 × 10
Total beam power loss (MW)	300	320
Peak luminosity (10^{41} cm^{-2}s^{-1})	2 × 2.5	2 × 12.5

The final goal of generating a suitable beam of muons to be used in a TeV-scale muon collider is accomplished by the EXMP scenario based on a twin 200–500-GeV ERL system coupled to a twin 50-GeV FEL ERL system, with residual beam power loss (after recovery, and taking into account all losses of the electron beam and FEL photon beam) of about $\sim$300 MW, together with an outstanding few nm rad-normalised emittance of the muon beam at $\sim 10^{11}$ muon pairs per second.

An important consideration concerns the peak properties of the primary electron beams: the parameters listed in the table represent the state-of-the-art for electron beams, with a RMS normalised transverse emittance (0.4 π μm rad, round beam) quite consistent with the accelerated bunch charge (250 pC). Moreover, the value chosen for the beta function at the collision point (0.2 mm) is very close to state-of-the-art performances. This allows to match the spot size of the FEL photon beam down to $14 - 10$ nanometers. The power budget for the primary electron beams is set by the ERL efficiency, bringing up to $2 \times (40 - 50) = 80 - 100$ MW.

3.1. High Efficiency Hard X-ray FELs

The photon beam needed to achieve ultra high luminosity in the $e^- - \gamma$ collider is unique: it must carry an outstanding number of photons per pulse at the same repetition rate of the primary electron beam. It must also match the ultra tight focus spot size at the collision of the primary electron beam, set by its very short beta function value at the focus (hundreds of microns), in the range of a few tens of nanometers. The only radiation source capable of meeting these demanding requirements is an FEL driven by a dedicated ERL, and operated in SASE mode with tapering, as illustrated in reference [13]. Efficiency in the range of a few percent is achievable, to a number of photons per pulse, as listed in Table 1, according to photon energy. The partial coherence of the amplified FEL radiation also makes it possible to focus its photon beam down to nanometer spot sizes, as discussed in reference [14]. This is the second crucial property of FELs that makes it possible to foresee a luminosity for the $e^- - \gamma$ collider scenarios of up to $2 \times (2.5 - 12.5) \times 10^{41}$ cm^{-2}s^{-1}. The FEL beams considered in this study carry an impressive amount of photon beam power: running at 800 MHz in CW mode, the photon number per second exceeds 10^{21}. With photon energies in the range of tens to hundreds of keV, that means up to 100 MW of radiation beam power. Since the FEL efficiency, considering the special mode of FEL operation as illustrated in reference [13], is about 1%, the power carried by the electron beam driving the FEL must be of the order of 100 MW/0.01 = 10 GW, as listed in Table 1.

There are two main challenges on the FEL side: (a) focusing FEL beams down to 10 nm was demonstrated at about 10 keV of photon energy, while EXMP needs at least 60 keV of FEL photons, and (b) handling FEL beams at a very large average power likely implies splitting the photon beam by means of multiplexing on different beam lines, which are further taken to the interaction point with the electron beam from different polar angles. These issues need further studies and evaluations in order to design a feasible collision scenario.

3.2. Power Budget

To summarize the power budget of the primary electron beam to that of the FEL driving electron beam, we get a total beam power loss of 300–320 MW for the EXMP cases. An expected efficiency beam-to-plug, not smaller than 20%, in the range 20–40%, would set the AC power bill in the 0.35–1 GW range.

We should note that the power transferred from the primary colliding beams into the secondary beams of muon pairs, photons, and electron-positron pairs was quite negligible compared to the stored power into the colliding beams at the collision point. In the case of EXMP WP200, the muon pair beams (10^{11} per second at an average energy of 50 GeV) took out only 1 kW of beam power. The power taken by the back-scattered Compton gammas (8×10^{12} per second, at an average energy of 200 GeV) was 250 kW, and the power taken by the electron-positron pair (10^{16} per second at an average energy of 1 GeV) was about 1.6 MW. All of these are quite negligible with respect to the total power loss quoted in Table 1 (300 MW), which is dominated by ERL efficiency and FEL photons. Furthermore, the real estate on top of the underground whole LINAC bunker, which extended over about 6 km^2 (nearly 30 km length times 200 m wide), if covered by solar panels, would make the whole system almost self-sustained by about 900 MW AC power generated by sunlight.

4. Simulation Results for Muon Beams

The significant values concerning the emitted particles for the analysed working points are reported in Table 2. The MPP events were generated by means of the Whizard [15,16], and ran in such a way to take into account the incoming beam features.

Table 2. Emitted particle characteristics for the EXMP scheme at working points WP200 and WP500.

	EXMP WP200		EXMP WP500
E_{CM} (MeV)		346	
X		4.7×10^5	
σ_{tot}^{TPP} (mb)		19	
σ_{tot}^{ICS} (µb)		14.7	
σ_{tot}^{MPP} (nb)		216	
$\mathcal{N}_{e^\pm}$ (s^{-1})	$2 \times 4.8 \times 10^{15}$		$2 \times 2.4 \times 10^{16}$
$\mathcal{N}_{ICS}$ (s^{-1})	$2 \times 3.7 \times 10^{12}$		$2 \times 1.8 \times 10^{13}$
$\mathcal{N}_{\mu^\pm}$ (s^{-1})	$2 \times 5.4 \times 10^{10}$		$2 \times 2.7 \times 10^{11}$
$\epsilon_{x_\mu}^n$ (π nm rad)	4.7		3.3
$\mathcal{N}_{\mu^\pm}^{10\%}$	$2 \times 1.1 \times 10^{10}$		$2 \times 5.4 \times 10^{10}$
$\mathcal{N}_{\mu^\pm}^{10\%}/\epsilon_{x_\mu}^n$ (10^{18} m^{-1}s^{-1})	2×2.3		2×16.3

The muon beam transverse normalised emittance is also reported in Table 2 and the number of muons per second divided by the emittance, the crucial figure of merit, as suggested in [17], was calculated. The muon beam normalised transverse emittance value for the WP200 is 4.7 π nm rad and of 3.3 π nm rad for WP500: these values compare to the analytical prediction of Equation (6), giving 5.9 π nm rad and 4.6 π nm rad, respectively. The MPP features for the two working points are displayed in Figure 3.

Concerning WP200, the outstanding value of the transverse normalised emittance combined with the number of muon pair per second, returns the value $\mathcal{N}_{\mu^\pm}/\epsilon_{x_\mu}^n = 2 \times 1.2 \times 10^{19}$ m^{-1}s^{-1}. If we consider the muons around the energy distribution peak of 50–100 GeV corresponding to a 10% RMS relative energy spread, the 20% of the produced muons are selected (with a longitudinal emittance value of ∼4.5 mm). The above-mentioned coefficient corresponding to this selection is $\mathcal{N}_{\mu^\pm}^{10\%}/\epsilon_{x_\mu}^n = 2 \times 2.3 \times 10^{18}$ m^{-1}s^{-1}, is comparable with the best option of the Gamma Factory [18,19] combined with LEMMA [3], analysed in reference [17]. The corresponding value for WP500 is $\mathcal{N}_{\mu^\pm}^{10\%}/\epsilon_{x_\mu}^n = 2 \times 16.3 \times 10^{18}$ m^{-1}s^{-1}. The top line of Figure 4 shows the energy spectrum of the ICS photons produced in the collision. As expected, in a high electron recoil regime, the energy peaks at around 200 GeV and 500 GeV for WP200 and WP500, respectively. The TPP, which is the most probable collateral reaction, involves $2 \times 4.8 \times 10^{15}$ and $2 \times 2.4 \times 10^{16}$ primary electrons, still a small fraction of the total (2×10^{18} per second). Moreover, the bottom line of Figure 4 shows that most of the primary electrons involved in TTP would face a negligible energy loss since the e^+/e^- pairs are mainly generated at a very low energy (see middle line).

A useful characteristic of the EXMP layout shown in Figure 2 involves the possibility of accelerating muons in the same LINACs used to accelerate the two twin primary electron beams. This is possible thanks to the very small emittance of muons and the non-interacting muon-electron beams. Beam optics could rely on RF focusing, which would be effective both on muons and on electrons, and will be further analysed in future work. LINAC acceleration of muons would allow to bring them up rapidly to the TeV kinetic energy range requested by muon collider physics, just in a few passes (each EXMP pass is $400 - 1000$ GeV energy gain) through the LINAC twin system, using proper muon recirculation arcs.

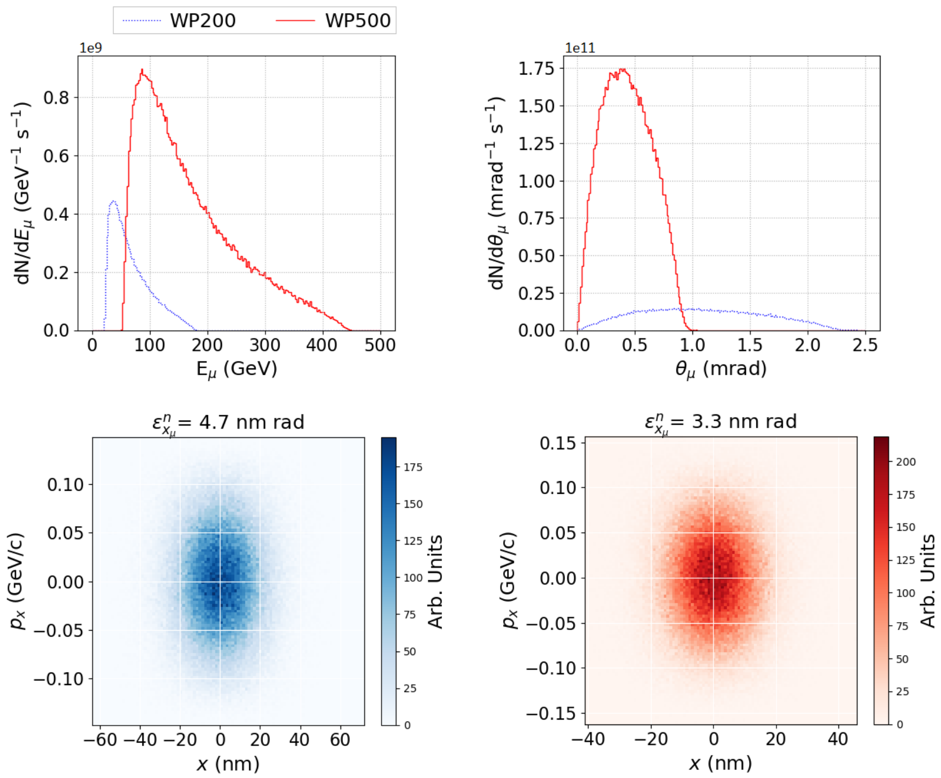

Figure 3. EXMP scheme: MPP features for WP200 (dotted blue) and WP500 (solid red). Muon beam energy spectra and angular distributions (top), phase space distribution in x and normalised x emittance (bottom).

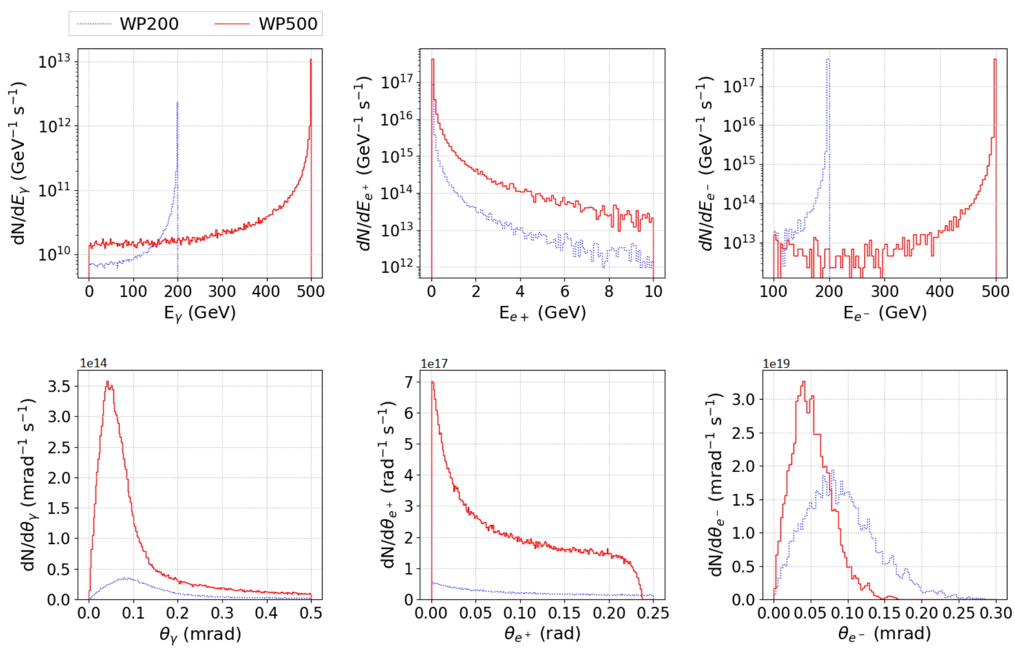

Figure 4. EXMP scheme: emitted ICS photon (column 1), TPP positron (column 2), and the initial electron beam after the TPP reaction (column 3) beam features for WP200 (dotted blue) and WP500 (solid red). Muon beam energy spectra (top) and angular distributions (bottom).

The effective laser parameter is $a_0 = 4.3\,\frac{\lambda_0}{w_0}\sqrt{U(J)/\sigma_t(ps)}$ with λ_0 the wavelength, w_0 the focal spot size, U the energy, and σ_t the RMS pulse length of the laser. In the assumption that the FEL beam behaves as a single mode, TEM_{00} laser mode, we checked that non-linear effects due to field intensity of the FEL photon beam could be considered negligible, since a_0, defining the non linearity of the electron-e.m. field interaction, is quite small, definitely below 10^{-2}. However, since EXMP is operated in a very large recoil regime (being X in excess of 10^5), the combination $\chi = a_0 X$ comes out to be much larger than 1, nearly 3×10^3. This is linked to the fact that the FEL e.m. field of the focused FEL beam is in the range of 10^{15} V/m, which, in the electron rest frame, is transformed to 10^{21} V/m, almost 3 orders of magnitude larger than Schwinger's limit. Further studies are needed to investigate potentials of this high recoil regime with respect to amplification of the electron-photon interaction strength.

5. PoP Experiment

We report in this section a possible option for a PoP experiment to be conducted at a facility where a GeV-class high brightness electron beam is operated, which could be possibly used parasitically for electron-photon collisions at E_{cm}, adequate for muon pair production. In order to replicate on a smaller scale the full scale EXMP scheme, a significant reduction in the electron beam energy (necessary to achieve a reasonable small scale PoP) must go along a proportional increase of the X-ray photon beam energy. Small emittance, a reasonable average current, and overall beam quality are other critical parameters to take into account. A natural example to consider is the European X-FEL, based at DESY, operating 17 GeV high brightness electron beams to drive the SASE X-ray FEL. Using an electron energy of 20 GeV, as a reference, the natural scaling of E_{cm} points to a photon energy of about 1.5 MeV (compared to 150 keV of the 200 GeV scenario described above). Therefore, a PoP experiment conducted at DESY with X-FEL would comprise the use of the spent electron beam emerging from the undulator, after an FEL radiation emission, colliding with an intense ICS gamma-ray beam of 1.5 MeV of photon energy. Such an ICS would be based on an SC-RF small LINAC of about 300 MeV energy, replicating the same time-structure of the X-FEL electron beam (10 Hz macro rep-rate with pulses 0.6 ms long carrying 2700 bunches 1 nC each, for an overall rep rate of 27 kHz). Up to 5×10^9 ICS photons per collision can be taken to the primary collision with the 20 GeV electrons, so to achieve the same $E_{cm} = 346$ MeV as the full-scale EXMP. Nearly 0.3 muon pairs per second can be generated, for $\sigma_0 = 2$ μm, with a transverse normalised emittance of 0.7 π μm rad (simulated value confirmed by the one predicted by formula 6 of 0.8 π μm rad) at a few GeV of average energy, as shown in Figure 5. Such a PoP would allow the characterization of the full 6D muon beam phase space, together with confirmation of the predicted cross section behavior as a function of E_{cm} (this can be easily adjusted by varying the ICS photon beam energy, as a LINAC-based ICS is tunable).

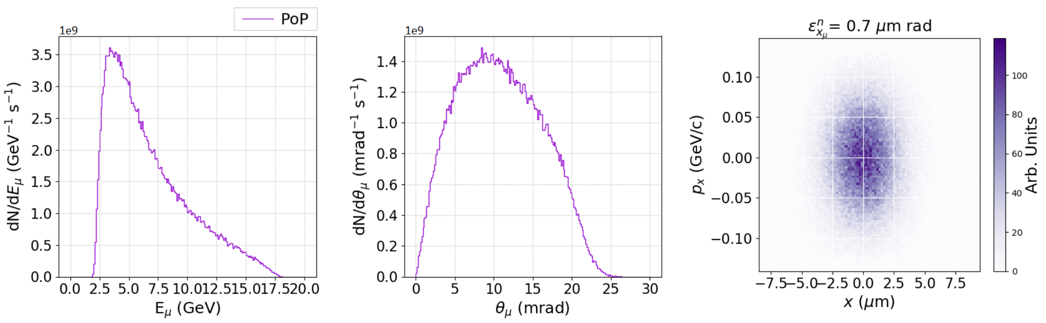

Figure 5. PoP for EXMP: MPP features. Muon beam energy spectra, angular distribution and phase space distribution in x.

6. Conclusions

We described a muon source based on electron-photon collisions at ultra-high luminosity, capable of reaching muon fluxes up to a few 10^{11} muon pairs per second at an outstanding normalised transverse emittance of a few nm rad, with muon beam energies peaking at 50–100 GeV. The electron-photon collider is based on a primary electron LINAC with energy in the 200–500 GeV range and a FEL LINAC driver with FEL photon energy in the 60–150 keV range. Extremely large beam power (both electron and photon beams) are needed to achieve the ultra-high luminosity, in excess of 10^{41} cm^{-2}s^{-1}. Since the electron-photon collisions transfer only a very small amount of power from the primary beams into the secondary beams, an efficient energy recovery must be implemented in the scenario, so as to reduce the amount of beam power loss down to the level of hundreds of MW, from 100 GW of beam power stored in the primary beams at collision. This is the main challenge of such a muon source, together with challenging beam collision spot sizes, in the range of a few tens of nanometers, and handling of an extremely large FEL photon beam power. The analysed scenario is based on a twin array of LINACs arranged face-to-face, providing both the primary electron beam and the FEL driving beam. It is of paramount importance to find a strategy of beam energy recovery with counterpropagating electron beams in the same LINAC. This was the original ERL layout conceived by M. Tigner a long time ago (see reference [20]), subject to R&D on twin super conducting cavities accommodating counterpropagating beams, but not yet demonstrated [21,22]. Further studies on the feasibility of these scenarios are necessary to assess the achievable luminosity of a muon collider based on this muon source, depending on the kind of accumulator scheme to combine with such a muon source scenario. The "promise" is to achieve the requested luminosity using much lower muon beam currents with respect to the other schemes, thanks to the very low emittances, which would significantly alleviate the issue of the muon beam-induced background. Additional potentialities are also to be studied and carefully analysed, e.g., the simultaneous acceleration of muon beams and primary electron beams in the main LINACs, possible polarization of muon beams if polarised primary electron beams are used (FEL photons are naturally polarized), parasitic use of intense GeV-class positron beams (up to 10^{16} pairs per second) generated in the electron-photon collisions, and of 100-GeV-class intense (in excess of 10^{12} per second) monochromatic photons. We are aware that the evaluations illustrated in this paper do not prove the feasibility of EXMP; they should be intended as guidelines-showing a roadmap towards a future feasibility study, followed by a conceptual design study.

Author Contributions: Conceptualization, investigation, writing-original draft preparation, writing-review and editing, C.C. and L.S. All authors have read and agreed to the published version of the manuscript.

Funding: This research received no external funding.

Conflicts of Interest: The authors declare no conflict of interest.

References

1. Muon Accelerator Program. Available online: https://map.fnal.gov (accessed on 5 January 2022).
2. MICE collaboration, Demonstration of cooling by the Muon Ionization Cooling Experiment. *Nature* **2020**, *578*, 53–59. [CrossRef] [PubMed]
3. Alesini, D.; Antonelli, M.; Biagini, M.E.; Boscolo, M.; Blanco-García, O.R.; Ciarma, A.; Cimino, R.; Iafrati, M.; Giribono, A.; Guiducci, S.; et al. Positron driven muon source for a muon collider. *arXiv* **2019**, arXiv:1905.05747v2.
4. Serafini, L.; Curatolo, C.; Petrillo, V. Low emittance pion beams generation from bright photons and relativistic protons. *arXiv* **2015**, arXiv:1507.06626v2.
5. Serafini, L.; Broggi, F.; Curatolo, C. Study of Hadron-Photon Colliders for Secondary Beam Generation. In Proceedings of the 8th International Particle Accelerator Conference (IPAC 2017), Copenhagen, Denmark, 14–19 May 2017; pp. 2865–2867.
6. Curatolo, C.; Broggi, F.; Serafini, L. Phase space analysis of secondary beams generated in hadron-photon collisions. *Nucl. Instrum. Methods Phys. Res. Sect. A* **2017**, *865*, 128–132. [CrossRef]
7. Motz, J.W.; Olsen, H.A.; Koch, H.W. Pair Production by Photons. *Rev. Mod. Phys.* **1969**, *41*, 632. [CrossRef]

8. Curatolo, C.; Drebot, I.; Petrillo, V.; Serafini, L. Analytical description of photon beam phase spaces in inverse Compton scattering sources. *Phys. Rev. Accel. Beams* **2017**, *20*, 080701. [CrossRef]
9. Angal-Kalinin, D.; Arduini, G.; Auchmann, B.; Bernauer, J.; Bogacz, A.; Bordry, F.; Bousson, S.; Bracco, C.; Brüning, O.; Calaga, R.; et al. PERLE. Powerful energy recovery linac for experiments. Conceptual design report. *J. Phys. G* **2018**, *45*, 065003. [CrossRef]
10. Klein, M.; Stocchi, A. PERLE: A High Power Energy Recovery Facility for Europe A contribution to the Update of the European Strategy on Particle Physics. 2018. Available online: http://cds.cern.ch/record/2652336 (accessed on 5 January 2022).
11. International Linear Collider. Available online: https://linearcollider.org/ (accessed on 5 January 2022).
12. Shiltsev, V.; Zimmermann, F. Modern and future colliders. *Rev. Mod. Phys.* **2021**, *93*, 015006. [CrossRef]
13. Emma, C.; Fang, K.; Wu, J.; Pellegrini, C. High efficiency, multiterawatt x-ray free electron lasers. *Phys. Rev. Accel. Beams* **2016**, *19*, 020705. [CrossRef]
14. Matsuyama, S.; Inoue, T.; Yamada, J.; Kim, J.; Yumoto, H.; Inubushi, Y.; Osaka, T.; Inoue, I.; Koyama, T.; Tono, K.; et al. Nanofocusing of X-ray free-electron laser using wavefront-corrected multilayer focusing mirrors. *Sci. Rep.* **2018**, *8*, 17440. [CrossRef] [PubMed]
15. Whizard. Available online: https://whizard.hepforge.org/ (accessed on 5 January 2022).
16. Kilian, W.; Ohl, T.; Reuter, J. WHIZARD: Simulating Multi-Particle Processes at LHC and ILC. *Eur. Phys. J.* **2011**, *C71*, 1742. [CrossRef]
17. Zimmermann, F. LHC/FCC-based muon colliders. *J. Phys.: Conf. Ser.* **2018**, *1067*, 022017. [CrossRef]
18. Krasny, M.W.; Antsiferov, P.S.; Apyan, A.; Alikhanyan, A.I.; Bessonov, E.G.; Shevelko, V.P.; Lebedev, P.N.; Budker, D.; Cassou, K.; Chaikovska, I.; et al. The CERN Gamma Factory initiative: An ultra-high intensity gamma source. In Proceedings of the 9th International Particle Accelerator Conference (IPAC'18), Vancouver, BC, Canada, 29 April–4 May 2018.
19. Płaczek, W.; Abramov, A.; Alden, S.E.; Alemany Fernandez, R.; Antsiferov, P.S.; Apyan, A.; Bartosik, H.; Bessonov, E.G.; Biancacci, N.; Jacek, B.; et al. The Gamma Factory Project at CERN: A New Generation of Research Tools Made of Light. *Acta Phys. Polon. Supp.* **2020**, *13*, 645–652. [CrossRef]
20. Tigner, M. A possible apparatus for electron clashing-beam experiments. *Il Nuovo Cimento* **1965**, *37*, 1228–1231. [CrossRef]
21. MariX. Available online: http://www.marix.eu/ (accessed on 5 January 2022).
22. Konoplev, I.; Ainsworth, R.; Burt, G.; Seryi, A. UH-FLUX: Compact, Energy Efficient Superconducting Asymmetric Energy Recovery LINAC for Ultra-high Fluxes of X-ray and THz Radiation. In Proceedings of the International Particle Accelerator Conference (IPAC'16), Busan, Korea, 8–13 May 2016.